Protective role of fermented mulberry leave extract in LPS-induced inflammation and autophagy of RAW264.7 macrophage cells

MI RIM LEE[1*], JI EUN KIM[1*], JIN JU PARK[1], JUN YOUNG CHOI[1], BO RAM SONG[1], YOUNG WHAN CHOI[2], DONG-SEOB KIM[3], KYUNG MI KIM[4], HYUN KEUN SONG[5] and DAE YOUN HWANG[1]

Departments of [1]Biomaterials Science, [2]Horticultural Life Sciences and [3]Food Science and Technology, College of Natural Resources and Life Science/Life and Industry Convergence Research Institute, Pusan National University, Miryang 50463; [4]Life Science Research Institute, Novarex Co., Ltd., Chungju 28126; [5]Central Research Institute, Kinesciences Co., Seoul 02850, Republic of Korea

Received November 25, 2019; Accepted May 18, 2020

DOI: 10.3892/mmr.2020.11563

Abstract. Mulberry leaves have antioxidant activity and anti-inflammatory effects in several types of cells. However, the efficacy of mulberry leaves fermented with *Cordyceps militaris* remains unknown. Therefore, the present study aimed to investigate whether the ethanol extracts of mulberry leaves fermented with *C. militaris* (EMfC) can prevent lipopolysaccharide (LPS)-induced inflammation and autophagy in macrophages. To achieve this, RAW264.7 cells pretreated with three different dose of EMfCs were subsequently stimulated with LPS, and examined for alterations in the regulatory factors of inflammatory responses and key parameters of the autophagy signaling pathway. EMfC treatment inhibited the generation of reactive oxidative species; however, significant activity was observed for 2,2-diphenyl-1-picrylhydrazyl (DPPH) radical scavenging (IC_{50}=579.6703 mg/ml). Most regulatory factors in inflammatory responses were significantly inhibited following treatment with EMfC, without any significant cellular toxicity. EMfC-treated groups exhibited marked suppression of nitrogen oxide (NO) levels, mRNA expression levels of iNOS/COX-2, levels of all inflammatory cytokines (TNF-α, IL-1β and IL-6) and phosphorylation of MAPK members, as well as recovery of cell cycle progression. Furthermore, similar effects were observed in the LPS-induced autophagy signaling pathway of RAW264.7 cells. The expression levels of microtubule-associated protein 1A/1B-light chain 3 (LC3) and Beclin exhibited a dose-dependent decrease in the EMfC+LPS-treated groups compared with in the Vehicle+LPS-treated group, whereas the phosphorylation of PI3K and mTOR were enhanced in a dose-dependent manner in the same groups. Overall, the results of the present study provide evidence that exposure to EMfC protects against LPS-induced inflammation and autophagy in RAW264.7 cells. These results indicated that EMfC is a potential candidate for treatment of inflammatory diseases.

Correspondence to: Professor Dae Youn Hwang, Department of Biomaterials Science, College of Natural Resources and Life Science/Life and Industry Convergence Research Institute, Pusan National University, Miryang 50463, Republic of Korea
E-mail: dyhwang@pusan.ac.kr

Professor Hyun Keun Song, Central Research Institute, Kinesiences Co., F1, Milovany, 28, Goryeodea-ro, Seongbuk-gu, Seoul 02850, Republic of Korea
E-mail: kali71@hanmail.net

*Contributed equally

Key words: mulberry leaves, *Cordyceps militaris*, inflammation, autophagy, MAPK pathway, PI3K/mTOR pathway

Introduction

The immune system is the body's natural defense mechanism against pathogens such as viruses, bacteria, and other intermediates (1). Inflammation occurs when a variety of harmful substances, ranging from infectious microorganisms (such as bacteria, viruses or fungi) to transgenic cells (such as cancer cells), reside in a specific tissue of the host or circulate in the blood (2-6). In response to reactions from these immune cells participating in inflammation are the inflammatory mediators, such as IL-1β and TNF-α, which are synthesized and secreted during an inflammatory response. Therefore, understanding the role of these inflammatory intermediaries and their associated mechanisms is one of the major goals for controlling the inflammatory response (5,6). Regulating the inflammatory response is critical in the treatment of inflammatory-related diseases such as systemic inflammatory response syndrome (SIRS), severe tissue damage, and septic shock. These inflammatory regulating agents include steroids, non-steroids and biological agents. However, development of new drugs are required to overcome certain drawbacks of the existing anti-inflammatory drugs, such as adverse side

effects and high prices (7). Recently, natural substances such as medicinal plants have drawn attention as resources for acquiring anti-inflammatory drugs that are easy to procure in large quantities at low cost, and are expected to have fewer side effects (8,9).

Morus alba, commonly known as mulberry in Korea, grows very well in a variety of climatic conditions, ranging from temperate areas to tropical areas, and is found in northern China, India, the Middle East, Southern Europe, and more recently in North America (10). Mulberry leaves are generally used to feed silkworms, and they contain numerous active compounds that possess various pharmacological activities (11). Many studies have reported the anti-bacterial, anti-oxidant, anti-hypoglycemic, anti-cancer, anti-obesity, anti-ER stress, and anti-inflammatory activities of the roots and shells (9,12-16). Especially, extracts of mulberry leaves fermented with *C. militaris* (EMfC) treatment is reported to inhibit fat accumulation in the HFD-induced obese C57BL/6 mice through regulation of lipogenesis and lipolysis (17). These effects of EMfC are tightly correlated with the suppression of ER stress and ER stress-induced apoptosis (18).

C. militaris, an insect pathogen belonging to Ascomycota, is traditionally used for elevating the immune response, and as an anti-cancer and anti-aging agent in Chinese and East Asian medicine (19). Several studies report that the cordycepin isolated from *C. militaris* has pharmacological activity as an anti-cancer (20), anti-bacterial (21), and anti-oxidant (22) agent. Similar effects have been reported for mixtures of *C. militaris* and secondary metabolite products secreted from mushrooms (23). We therefore hypothesized that certain products of mulberry leaves fermented with *C. militaris* would exert protection against an lipopolysaccharide (LPS)-induced inflammatory response and the autophagy pathway.

In the current study, we examined the basic mechanisms involved in the anti-inflammatory and anti-autophagic activity of EMfC in LPS-stimulated RAW264.7 macrophage cells. Our results provide new data indicating that EMfC is associated with the prevention of inflammation and autophagy-related diseases via the regulation of iNOS-mediated COX-2 induced pathway, MAPK signaling pathways, and PI3K/mTOR pathway.

Materials and methods

Cell culture. RAW264.7 cells (ATCC) were cultured in Dulbecco Modified Eagle's Medium (DMEM; Thermo Fisher Scientific, Inc.) supplemented with 10% fetal bovine serum (FBS; Welgene), L-glutamine, penicillin, and streptomycin (Thermo Fisher Scientific, Inc.), in a humidified incubator at 37˚C under 5% CO_2 and 95% air.

Preparation of EMfCs. EMfC samples were prepared in accordance with a previous papers (17). The samples of mulberry leaves were collected in October 2015 from plantations in the Sangju district of Korea, and characterized by Professor Young Whan Choi at the Department of Horticultural Bioscience, Pusan National University. Voucher specimens of mulberry leaves were deposited in the herbarium (accession no. Mul-PDRL-1) of the Pusan National University (Miryang, Korea). The *C. militaris* used for fermentation was kindly provided by Professor Sang Mong Lee of the Department of Life Science and Environmental Biochemistry, Pusan National University. The Jeongeup Agriculture Cooperative Federations for Silkworm Farming (Jeongeup, Korea) supplied the silkworm pupae powder.

Briefly, fresh mulberry leaves were first completely dried in a hot-air drying machine (JSR) for 24 h at 60˚C, and subsequently powdered using an electric blender. The powdered dried mulberry leaves were sterilized by autoclaving at 121˚C for 60 min, and mixed with 50% silkworm powder (SWP). This mixture was inoculated with 10% *C. militaris* (v/w) and incubated in a shaking incubator (#SI-600R; Lab Companion) maintained at 150 rpm and 25˚C, and fermented for 4 weeks. Subsequently, the pellet of fermented mixture was harvested by centrifuging the flask at 3,000 rpm for 10 min. To prepare the extracts of fermented mulberry powder, the harvested pellet was mixed with the solvent (95% EtOH) in a fixed liquid ratio (mulberry powder:solvent, ratio 1:10), and sonicated for 1 h using a JAC ultrasonic device (KODO). This sonicated pellet was collected using centrifugation at 3,000 rpm for 10 min. The resultant pellet was resuspended in 9 ml of the solvent, and further sonicated using the same conditions. This procedure was repeated once more, and the resultant supernatant was collected, filtered through a 0.4 μm filter (#HAWP04700, Millex-LH; Merck Millipore), and evaporated using a vacuum evaporator (#R-300; BUCHI Corporation). Finally, lyophilization of the EMfC was achieved using a circulating extraction equipment (IKA Labortechnik). The extracts were dissolved in DMSO (#D2660; Sigma-Aldrich; Merck KGaA) at a concentration of 50 mg/ml before use.

Scavenging activity of free radical. The scavenging capability of the 2,2-diphenyl-1-picrylhydrazyl (DPPH) radical was measured at eight different concentrations of EMfC (0-1,000 μg/ml), according to the method described in a previous study (24). Briefly, each sample of EMfC (100 μl) was mixed with 100 μl of 0.1 mM DPPH (Sigma-Aldrich; Merck KGaA) prepared in 50% DMSO solution. After 30 min of incubation at room temperature, absorbance of the reaction mixture was recorded using a Versa-max plate reader (Molecular Devices) at a wavelength of 517 nm. The percent drop in the absorbance, relative to that of the control, determined the DPPH radical scavenging activity of the EMfC. The concentration of EMfC resulting in a 50% loss in DPPH activity was determined to be the IC_{50}.

Cell viability assay. Cell viability was determined using the tetrazolium compound 3-[4,5-dimethylthiazol-2-yl]-2,5-diphenyltetrazolium bromide (MTT) (Sigma-Aldrich; Merck KGaA) assay. Briefly, RAW264.7 cells were seeded at a density of $2x10^4$ cells/0.2 ml medium per well, and incubated for 24 h in a humidified CO_2 incubator at 37˚C. On attaining 70-80% confluency, each well was assigned to one of the five experimental groups: Untreated group, Vehicle+LPS treated group, EMfCLo+LPS (low concentration of EMfC, 100 μg/ml) treated group, EMfCMid+LPS (medium concentration of EMfC, 200 μg/ml) treated group, and EMfCHi+LPS (high concentration of EMfC, 400 μg/ml) treated group. The cells were exposed to either DMSO (Vehicle+LPS treated group) or

the assigned concentration of EMfC for 2 h, and subsequently stimulated with 1 μg/ml LPS (Sigma-Aldrich; Merck KGaA) for 24 h in a 37˚C incubator. The supernatants were subsequently discarded, and 0.2 ml of fresh DMEM was added to each well, followed by addition of 50 μl of MTT solution (2 mg/ml in 1X PBS). The cells were incubated at 37˚C for 4 h, after which the MTT was removed and cells were lysed by adding 150 μl DMSO/well. The optical density was measured at 570 nm using a microplate reader (Molecular Devices VERSA max Plate reader). The morphological features of RAW264.7 cells in each treated group were also observed using a light microscope (Leica Microsystems).

Analysis of intracellular reactive oxygen species (ROS) level. ROS levels were measured by staining with 2',7'-dichlorofluorescein diacetate (DCFH-DA) (Sigma-Aldrich; Merck KGaA). Briefly, RAW264.7 cells were seeded at a density of $1x10^5$ cells/ml in 24-well plates for 24 h, and exposed to three different concentrations of EMfC (100, 200 or 400 μg/ml) or DMSO for 2 h in a 37˚C incubator. The cells were subsequently stimulated with 1 μg/ml LPS for further 24 h. Cells were then incubated with 25 μM DCFH-DA for 30 min at 37˚C, washed twice with PBS, and observed for green fluorescence at x200 magnification using a fluorescent microscope (Eclipse TX100; Nikon).

Nitrogen oxide (NO) concentration analysis. NO concentration in the culture supernatant was measured using Griess reagent (1% sulfanilamide, 5% phosphoric acid, 0.1% N-(1-naphthyl) ethylenediamine dihydrochloride; Sigma-Aldrich; Merck KGaA), as described previously (25,26). Briefly, RAW264.7 cells were treated with vehicle or EMfC (100, 200 or 400 μg/ml) for 2 h, followed by LPS stimulation (1 μg/ml) and incubation for 24 h. After harvesting the culture supernatant, each sample (100 μl) was mixed with the same volume of Griess reagent, and incubated at room temperature for 10 min. Absorbance was read at 540 nm using a VersaMax microplate reader (Molecular Devices). The concentration of NO in the cell culture fluid was calculated by comparing with a standard curve of sodium nitrite ($NaNO_2$).

Reverse transcription-quantitative (RT-q)PCR analysis for cytokine gene expression. Total RNA was isolated by cell lysis using RNAzol CS104 (Tel-Test Inc.), followed by cell reverse transcription and PCR. Next, 10 pmol of the sense and antisense primers were added, and the reaction mixture was subjected to 28-32 cycles of amplification, conducted in a Perkin-Elmer Thermal Cycler, using the following cycle: 30 sec at 94˚C, 30 sec at 62˚C, and 45 sec at 72˚C. The primer sequences used for target gene expression identification were as follows: iNOS, sense, 5'-CACTTGGAGTTCACCCAGT-3' and antisense primer, 5'-ACCACTCGTACTTGGGATGC-3'; COX-2, sense, 5'-GAGGTGTATC-3', antisense primer, 5'-CCA GGAGGATGGAGTTGTTGTAGAG-3'; TNF-α, sense, 5'-CCTGTAGCCCACGTCGTAGC-3' and antisense primer, 5'-TTGACCTCAGCGCTGACTTG-3'; IL-1β, sense, 5'-GCA CATCAACAAGAGCTTCAGGCAG-3' and antisense primer, 5'-GCTGCTTGTGAGGTGCTGATGTAC-3'; IL-6, sense, 5'-TTGGGACTGATGTTGTTGACA-3' and antisense primer, 5'-TCATCGCTGTTGATACAATCAGA-3'. The experiment was repeated three times, and all samples were analyzed in triplicate. The final PCR products were separated on 1-2% agarose gel and visualized by ethidium bromide staining. The density of specific bands was quantified using a Kodak Electrophoresis Documentation and Analysis System 120 (Eastman Kodak).

RT-qPCR analysis for cytokine gene expression. RAW264.7 cells were homogenized with Polytron PT-MR 3100 D Homogenizer (Kinematica AG) in TRIzol (Invitrogen; Thermo Fisher Scientific, Inc.), as per the manufacture's protocol. After ethanol precipitation, total RNAs were harvested by centrifugation at 10,000 x g for 15 min, and their concentration was subsequently determined using the Nano-300 Micro-Spectrophotometer (Allsheng Instruments Co., Ltd.). Total complementary DNA (cDNA) against mRNA was synthesized using 200 units of SuperScript II reverse transcriptase (Thermo Fisher Scientific, Inc.). RT-qPCR was conducted with the cDNA template (1 μl), 2X Power SYBR Green (6 μl; Toyobo Life Science), and specific primers used in the RT-PCR analysis in appropriate buffer solution. The cycle quantification value (Cq) was determined as described in the Livak and Schmittgen's method (27).

Enzyme-linked immunosorbent assay (ELISA) for IL-6 cytokine. Cells were pretreated with either Vehicle (DMSO) or different concentrations of EMfC (100, 200 or 400 μg/ml) for 1 h, prior to stimulation with 1 μg/ml LPS for 24 h. The culture supernatant of RAW264.7 cells was assayed for IL-6 using an IL-6 ELISA kit (Biolegend), according to the manufacturer's instructions.

Western blot analysis. RAW264.7 cells were treated with Vehicle (DMSO) or EMfC (100, 200 or 400 μg/ml) for 2 h, followed by 1 μg/ml LPS stimulation for 15 min. The treated cells were lysed using the Pro-Prep Protein Extraction Solution (iNtRON Biotechnology). The cell lysate was centrifuged at 13,000 rpm for 5 min, and concentration of total protein was quantified using the SMARTTM BCA Protein Assay Kit (Thermo Fisher Scientific, Inc.). The proteins were separated by 4-20% sodium dodecyl sulfate-polyacrylamide gel electrophoresis (SDS-PAGE) for 2 h. The gels were transferred to nitrocellulose membranes for 2 h at 40 V. The membranes were subsequently blocked by incubating with 3% skim milk for 1 h at room temperature. Each membrane was then incubated separately, overnight at 4˚C, with the following primary antibodies: Anti-SAPK/JNK (Cell Signaling Technology), anti-p-SAPK/JNK (Thr183/Tyr185) (Cell Signaling Technology), anti-ERK (K-23) (Santa Cruz Biotechnology), anti-p-ERK (E-4) (Santa Cruz Biotechnology), anti-p38 MAPK (Cell Signaling Technology), anti-p-p38 MAP Kinase (Thr180/Tyr182) (Cell Signaling Technology), anti-PI3K (Cell Signaling Technology), anti-p-PI3K (Cell Signaling Technology), anti-mTOR (Cell Signaling Technology), anti-p-mTOR (Cell Signaling Technology), anti-LC3 (Cell Signaling Technology), anti-Beclin (Cell Signaling Technology), and anti-β actin (Sigma-Aldrich; Merck KGaA). The probed membranes were then washed with washing buffer (137 mM NaCl, 2.7 mM KCl, 10 mM Na_2HPO_4, and 0.05% Tween-20) and subsequently incubated with 1:1,000 diluted horseradish peroxidase (HRP)-conjugated goat anti-rabbit IgG secondary

antibody (Invitrogen; Thermo Fisher Scientific, Inc.), at room temperature for 1 h. Finally, membrane blots were developed using the Amersham ECL Select Western Blotting detection reagent (GE Healthcare). The chemiluminescence signals that originated from the specific bands were detected using FluorChemi®FC2 (Alpha Innotech Co.).

Autophagic vacuole analyses. For analyzing autophagic vacuoles, the cells were treated similar to previous experiments, and subsequently washed and stained using the Autophagy LC3-antibody-based kit (Millipore), according to the manufacturer's instructions. The cells were incubated with Autophagy Reagent A in Earle's balanced salt solution (EBSS) for 5 h at 37˚C, followed by washing with ice cold HBSS. The cells were then stained with anti-LC3 Alexa Fluor® 555 in 1X Autophagy Reagent B on ice for 30 min in the dark, and washed with ice cold 1X Assay Buffer. The stained samples were quantified by flow cytometry using a Muse Cell Analyzer (Millipore) in duplicates. Based on manufacture's instruction, at least 1,000 events for each sample should be acquired to assure statistically significant determination of stained cells number. These quantified results were presented as autophagy induction ratio (test sample fluorescence relative to control) after analysis using the MuseSoft 1.4.0.0. software.

Statistical analysis. One-way ANOVA (SPSS for Windows, Release 10.10; Standard Version; SPSS Inc.) followed by Tukey's post hoc test, was used to identify significant differences between the Vehicle and the EMfC treated groups. All values are reported as the means ± SD, and $P<0.05$ is considered to indicate a statistically significant difference.

Results

Antioxidant ability of EMfC. To evaluate the antioxidant ability of EMfC, we measured the DPPH scavenging activity and ability to suppress ROS production at varying concentrations of EMfC and LPS-stimulated RAW264.7 cells. As shown in Fig. 1A, the inhibitory activity against DPPH radicals gradually increases dose-dependently from 1-1,000 μg/ml EMfC, with an IC_{50} value of 579.6703 μg/ml. Also, treatment of EMfC shows strong antioxidant activity at serial concentrations that reduce the level of ROS production during the inflammatory response of macrophages induced by LPS (Fig. 1B). These results indicate that subsequent to LPS stimulation, the therapeutic function of EMfC in RAW264.7 cells is probably associated with antioxidant activity.

Inhibitory effects of EMfC on the LPS-induced inflammatory response in RAW264.7 cells. To investigate whether exposure to EMfC prevents the LPS-induced inflammatory response, alterations in the NO concentration, the mRNA expressions of iNOS/COX-2 and inflammatory cytokines (TNF-α, IL-6 and IL-1β), phosphorylation of MAPK pathway members, and cell numbers at each stage of the cell cycle, were measured in RAW264.7 cells pretreated with three different doses of EMfCs and subsequently stimulated with LPS. Until now, it is well known that the NO produced by iNOS (especially the active oxygen species produced during inflammatory responses in LPS-stimulated macrophages) plays an important role as a mediator in the inflammatory response. As shown in Fig. 2B, exposure to EMfC dramatically reduces the level of NO in the inflammatory response of LPS-stimulated macrophages, without any significant cell toxicity (Fig. 2A). Also, treatment with EMfC significantly increases the concentration of NO in LPS-induced macrophages in the Vehicle+LPS group, as compared to that of the Untreated group. However, as compared to the Vehicle+LPS group, the NO concentration of cells pretreated with EMfCMi and EMfCHi show significantly reduced NO levels, whereas the EMfCLo treated group shows similar NO levels (Fig. 2B). Furthermore, RT-PCR and RT-qPCR were applied to examine alterations in the iNOS-mediated COX-2 induced pathway in EMfC+LPS treated cells. Enhanced levels of iNOS and COX-2 mRNA were detected in the Vehicle+LPS group as compared to the Untreated groups. Especially, these increased expression levels of iNOS and COX-2 mRNA were strongly reduced after exposure to EMfC, as compared to the Vehicle+LPS group (Fig. 2C and D).

Moreover, RT-PCR analysis for inflammatory cytokine mRNA revealed that LPS stimulation induces a significant increase in the generation of TNF-α, IL-6 and IL-1β mRNA in RAW264.7 cells treated with Vehicle+LPS, as compared to controls (Untreated group). However, compared to the Vehicle+LPS treated group, the mRNA levels of these cytokines in the EMfC+LPS treated groups were significantly reduced in a dose-dependent manner (Fig. 3A). A dose-dependent reduction of IL-6 was also observed in protein production in the IL-6 ELISA assay (Fig. 3B). Similar results of inflammatory cytokine expressions were obtained by RT-qPCR analysis (Fig. 3C).

A typical signal transduction involved in inflammation is the MAPK pathway. This pathway is reportedly involved in inflammatory cytokine expression, control of cell response to stress, cell growth, and differentiation. In an inflammatory response, the MAPK signaling pathway plays a crucial role in regulating the inflammatory cytokines. To investigate the relationship between EMfC function and MAPK pathways, the phosphorylation levels of ERK, JNK and p38 were evaluated in macrophages exposed to EMfC and stimulated with LPS. As presented in Fig. 4, phosphorylation levels of ERK, JNK and p38 increase significantly after LPS treatment in the Vehicle+LPS group, as compared to the Untreated group. However, administration of EMfC to LPS-stimulated RAW264.7 cells significantly inhibits the phosphorylation of ERK, JNK and p38, as compared to the Vehicle+LPS group.

We further examined whether the suppression effect of EMfC reflects on the cell cycle arrest in RAW264.7 cells, pretreated at each concentration followed by induction of an inflammatory response with LPS. As shown in Fig. 5, the S phase of the LPS-treated inflammation in the Vehicle+LPS group decreases from 16.8 to 7.2%, the G1 phase increases from 46.1 to 70.3%, and the G2/M phase decreases from 37.1 to 22.5%. These results suggest that a G1 arrest is caused by the LPS-stimulated inflammatory reaction. Contrarily, the G1 cycles in cells exposed from low to high EMfC concentrations were 59.6, 53.6 and 51.7% respectively, compared to the Vehicle+LPS group, and show minimal changes in the S phase.

Taken together, our results suggest that EMfC prevents the LPS-induced inflammatory response through regulation

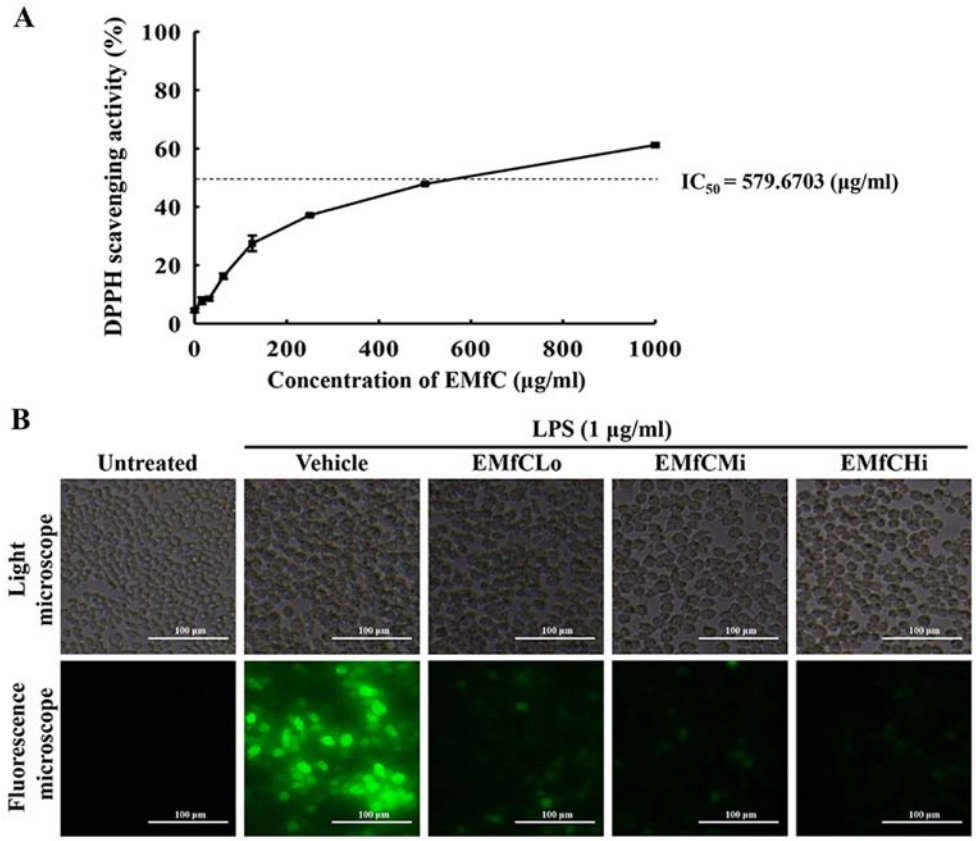

Figure 1. Determination of DPPH radical scavenging activity and intracellular ROS production. (A) DPPH radical scavenging activity of EMfC was assayed in a mixture containing 0.1 mM DPPH and varying concentrations of EMfC (0-1,000 μg/ml). For each dose, two to three wells were evaluated, and the optical density was measured in duplicate for each sample. (B) Determination of intracellular ROS production. Following DCFH-DA treatment of EMfC+LPS-treated RAW264.7 cells, green fluorescence was examined in the subset groups of cells using a fluorescence microscope. Magnification, x200. DPPH, 2,2-diphenyl-1-picrylhydrazyl; EMfC, ethanol extracts of mulberry leaves fermented with *C. militaris*; LPS, lipopolysaccharide; ROS, reactive oxygen species; Lo, low; Mi, medium; Hi, high.

of the iNOS-mediated COX-2 induced pathway, inflammatory cytokine transcription, MAPK signaling pathway, and cell cycle arrest.

Suppression effects of EMfC on the LPS-induced autophagy pathway in RAW264.7 cells. Several studies have reported the involvement of autophagy in LPS-induced inflammation. Therefore, to determine whether EMfC affects the autophagy pathway, we measured the surface and total cellular expression of LC3 using the anti-LC3 antibody, in LPS-stimulated RAW264.7 macrophages exposed to different concentrations of EMfC. As shown in Fig. 6A, the LC3 level on the cell surface is remarkably enhanced by LPS stimulation in the Vehicle+LPS group, as compared to the Untreated group. However, a dose-dependent inhibition was observed after exposure to EMfC. Also, Western blot analysis revealed similar inhibition patterns for the total cellular expression of LC3 (Fig. 6B). These results indicate that EMfC inhibits the LPS-induced autophagy.

To determine the signal transduction mechanism that inhibits the autophagy generation in LPS-stimulated macrophages by EMfC, we measured the phosphorylation of PI3K and mTOR, and production of Beclin protein using Western blot analysis. As seen in Fig. 6C, the phosphorylation levels of PI3K and mTOR in LPS-stimulated RAW264.7 cells are significantly reduced in the Vehicle+LPS group, compared to controls (Untreated group). However, the phosphorylation of PI3K and mTOR are strongly upregulated in a dose-dependent manner after EMfC treatment. The expression of Beclin, controlled by PI3K activation, is strongly increased in the Vehicle+LPS group, where phosphorylation of PI3K and mTOR is reduced after LPS exposure; as expected, Beclin levels decrease with increasing phosphorylation of PI3K and mTOR after EMfC exposure. These results indicate that EMfC inhibits the LPS-induced autophagy via the regulation of PI3K/mTOR pathway in RAW264.7 cells.

Discussion

Fermentation is the process wherein microbes produce substances that are useful to humans (28). Traditionally, many foods have been developed by fermentation, and numerous studies have proved the beneficial effects of these fermented foods on health, by improving the absorption rate of food and physiological activity of food components. Recent studies have drawn attention of applying these fermentation techniques to natural products, for obtaining more useful and improved physiological activities. For example, fermentation of red ginseng facilitates intraperitoneal absorption by converting saponin, the main component of red ginseng, into low-molecular weight material (29). In addition to increasing the absorption rate, the study also found that fermentation enhances the

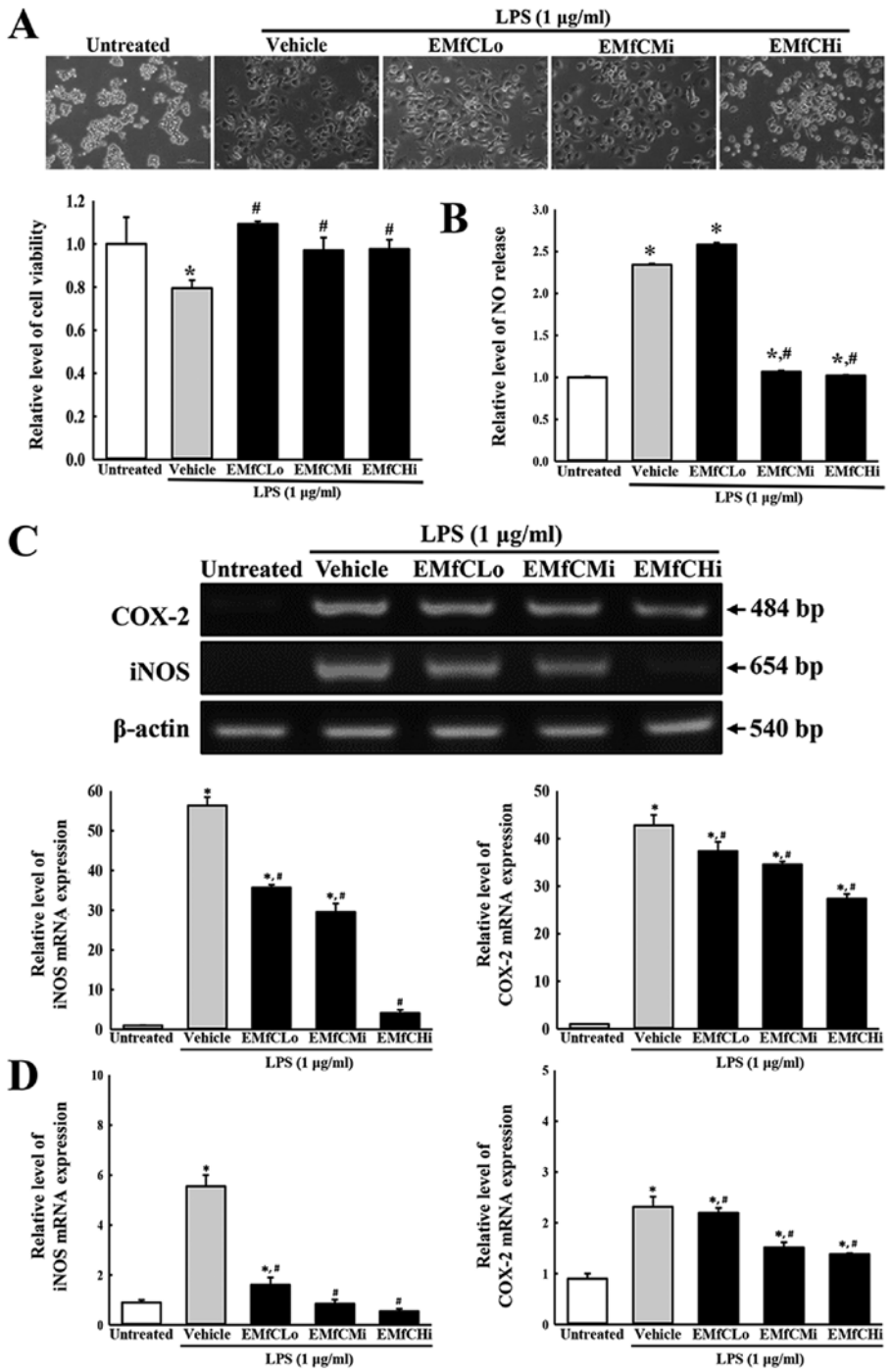

Figure 2. Determination of cytotoxicity, NO production and iNOS/COX-2 transcription. (A) Cytotoxicity of EMfC. LPS-treated RAW264.7 cells were incubated in the absence or presence of EMfC (100, 200 and 400 μg/ml) for 24 h. Cell morphology was observed under a microscope. Magnification, x200. Cell viability was estimated using the MTT assay. For each group, two to three wells were used in the MTT assay, and optical density was measured in duplicate for each sample. (B) NO production. RAW264.7 cells ($5x10^5$ cells/ml) were treated with the Vehicle or the indicated concentrations of EMfC, in the absence or presence of LPS (1 μg/ml) for 24 h. The supernatants were subsequently isolated and analyzed for nitrite. NO production was determined by measuring nitrite accumulation in the culture medium using the Griess reaction. For each group, two to three wells were used in the preparation of culture supernatant, and the Griess reaction was performed in duplicate for each sample. (C) Transcription levels of iNOS/COX-2. Alterations in the levels of COX-2 and iNOS were measured by RT-PCR. After the intensity of each band was determined using an imaging densitometer, the relative levels of COX-2 and iNOS mRNA were calculated based on the intensity of actin. (D) Quantification of iNOS/COX-2 transcripts using RT-qPCR. For each group, two to three wells were used in the preparation of total RNA, and RT-PCR and RT-qPCR analysis was performed in duplicate for each sample. Data are presented as the mean ± SD. *P<0.05 vs. Untreated group; $^\#$P<0.05 vs. Vehicle+LPS-treated group. NO, nitrogen oxide; COX-2, cyclooxygenase-2; iNOS, nitric oxide synthase; EMfC, ethanol extracts of mulberry leaves fermented with *C. militaris*; LPS, lipopolysaccharide; RT-qPCR, reverse transcription-quantitative PCR; Lo, low; Mi, medium; Hi, high.

anti-inflammatory and antioxidant activity of red ginseng (30). In another example, fermented cultures using mushrooms such as *Schizophyllum commune*, are reported to augment the antioxidant and anti-inflammatory effects as compared to unfermented mushrooms (31). A study on fermented *C. militaris* reported the beneficial effects for hypertension (32). Choi and Hwang (33) showed that the anti-inflammatory activity of mulberry leaves is due to the reduction of NO

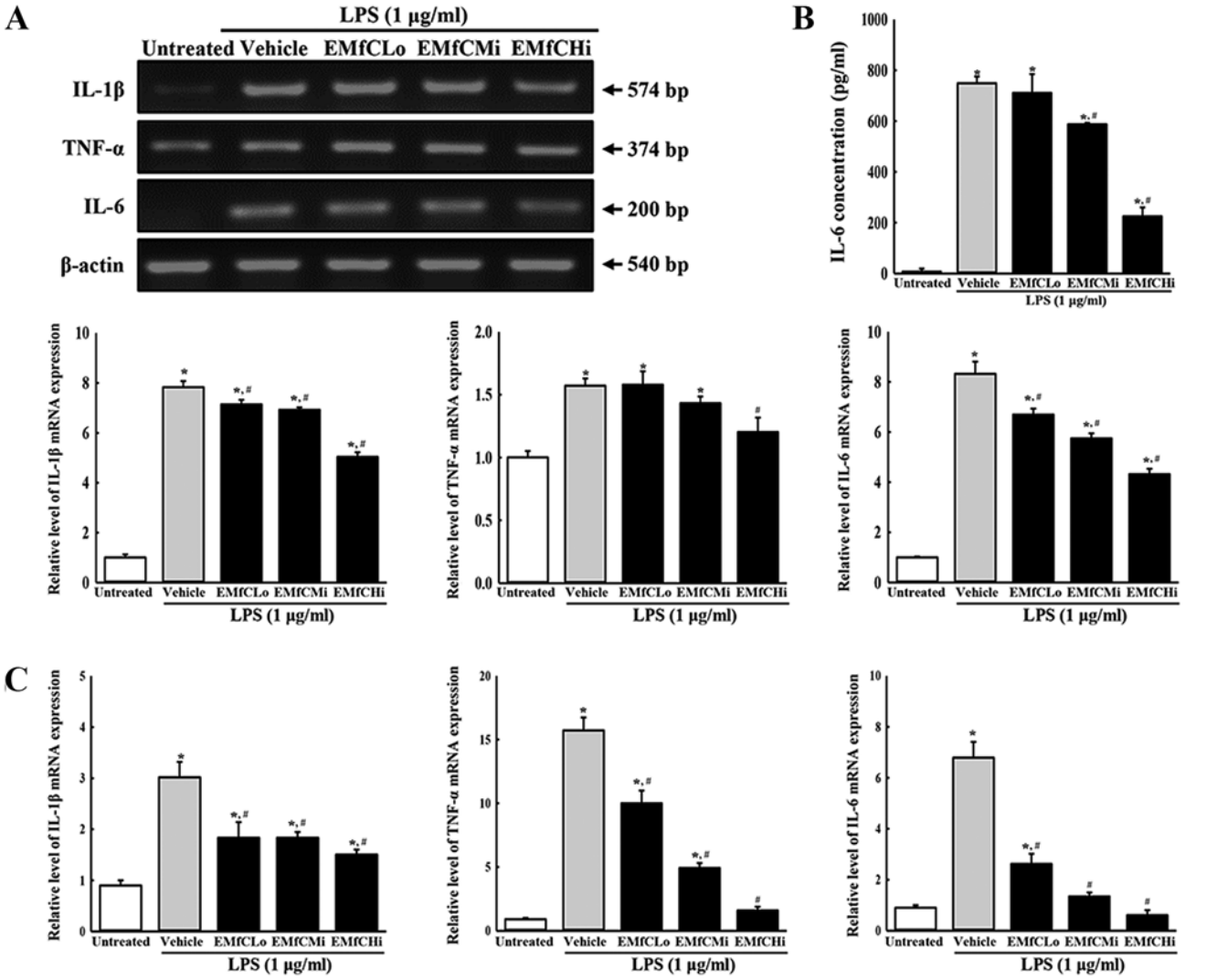

Figure 3. Determination of inflammatory cytokine levels. (A) Transcription levels of inflammatory cytokines. LPS-stimulated RAW264.7 cells were treated with either Vehicle or varying concentrations of EMfC for 3 h, and the mRNA expression levels of TNF-α, IL-1β and IL-6 were determined by RT-PCR. After the intensity of each band was determined using an imaging densitometer, the relative mRNA expression levels of TNF-α, IL-1β and IL-6 were calculated based on the intensity of actin. (B) Secreted protein levels of IL-6. Alterations in the levels of IL-6 protein in culture supernatants of differently treated RAW264.7 cells were measured by ELISA. (C) Quantification of IL-1β, TNF-α and IL-6 transcripts using RT-qPCR. For each group, two to three wells were used in the preparation of total RNA and culture supernatant, and RT-PCR, ELISA and RT-qPCR analysis was performed in duplicate for each sample. Data are presented as the mean ± SD. *P<0.05 vs. Untreated group; #P<0.05 vs. Vehicle+LPS-treated group. EMfC, ethanol extracts of mulberry leaves fermented with *C. militaris*; LPS, lipopolysaccharide; RT-qPCR, reverse transcription-quantitative PCR; Lo, low; Mi, medium; Hi, high.

and alteration in the levels of cytokines. In the current study, we evaluated the anti-inflammatory and anti-autophagy activities of mulberry leaves fermented by *C. militaris*, and determined the effects on NO production, iNOS-mediated COX-2 induced pathway, inflammatory cytokines transcription, MAPK pathway, cell cycle arrest, autophagic vacuole, and PI3K/mTOR pathway in LPS-stimulated RAW264.7 cells exposed to the fermented product.

Oxidative stress is a condition in which the balance of oxidative stimulators and inhibitors in the body is disturbed by events such as inflammation. This ultimately causes oxidative damage to cells and the human body. The active oxygen species involved in oxidative damage is ROS, especially NO, which is known to play a significant role in the inflammatory response (34). NO plays an important role in signal delivery and killing bacteria under normal conditions, but excessive NO production causes adverse side effects such as tissue damage and genetic mutations (35). Thus, antioxidants that inhibit oxidative stress by eliminating the active oxygen species (including NO) are important candidates as anti-inflammatory drugs. In this study, we observed a dose-dependent degradation of free radicals and NO generation in LPS-stimulated RAW264.7 cells after exposure to EMfC. No cell toxicity was observed at the EMfC concentrations exerting the antioxidant and NO production inhibitory effects. Moreover, EMfC also inhibited the expressions of iNOS and COX-2 during activation of iNOS-mediated COX-2 induced pathway.

Macrophages that engage in adaptive immunity as antigen presenting cells and are involved in adaptive immunity by inducing an inflammatory response by monitoring external substances, are important cells in charge of the front line of the immune system. In particular, during inflammatory reactions, macrophages express toll-like receptors (TLRs) on the surface to sensitize pathogens. TLR4 is responsible for the function

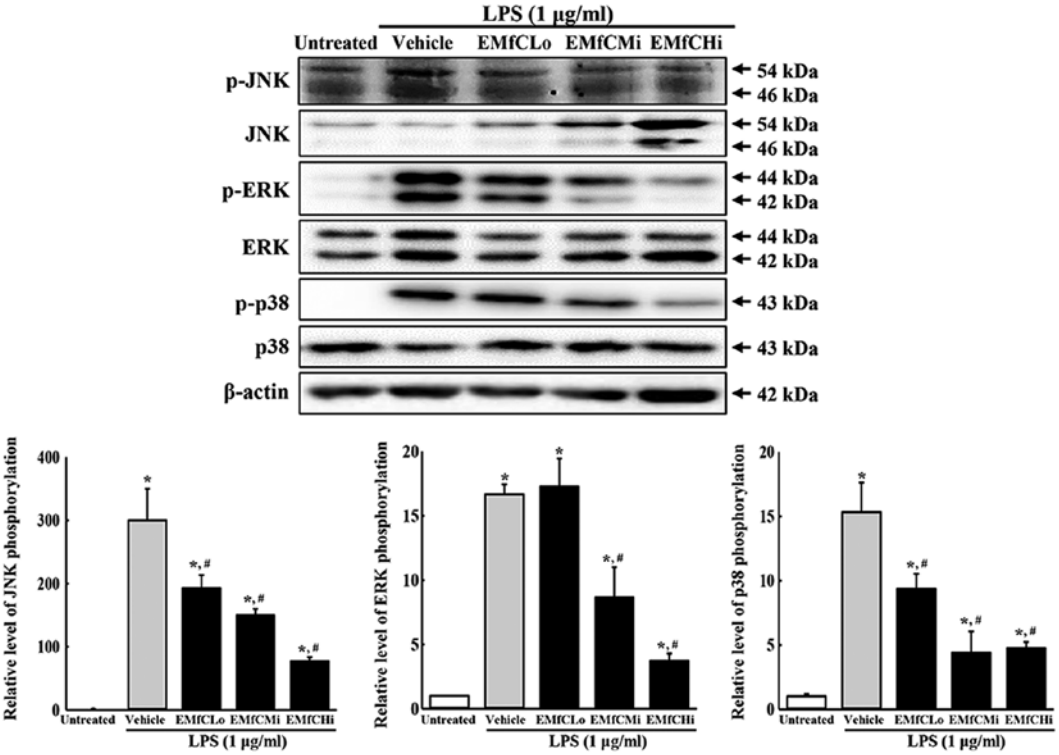

Figure 4. Detection of MAPK pathway. Alteration in the levels of p-PI3K/PI3K, p-mTOR/mTOR and β-actin proteins were measured by western blotting. After the intensity of each band was determined using an imaging densitometer, the relative levels of the six proteins were calculated, based on the intensity of actin protein. For each group, two to three dishes were used in the preparation of the cell homogenates, and western blot analysis was performed in duplicate for each sample. Data are presented as the mean ± SD. *P<0.05 vs. Untreated group; #P<0.05 vs. Vehicle+LPS-treated group. p-, phosphorylated; EMfC, ethanol extracts of mulberry leaves fermented with *C. militaris*; LPS, lipopolysaccharide; Lo, low; Mi, medium; Hi, high.

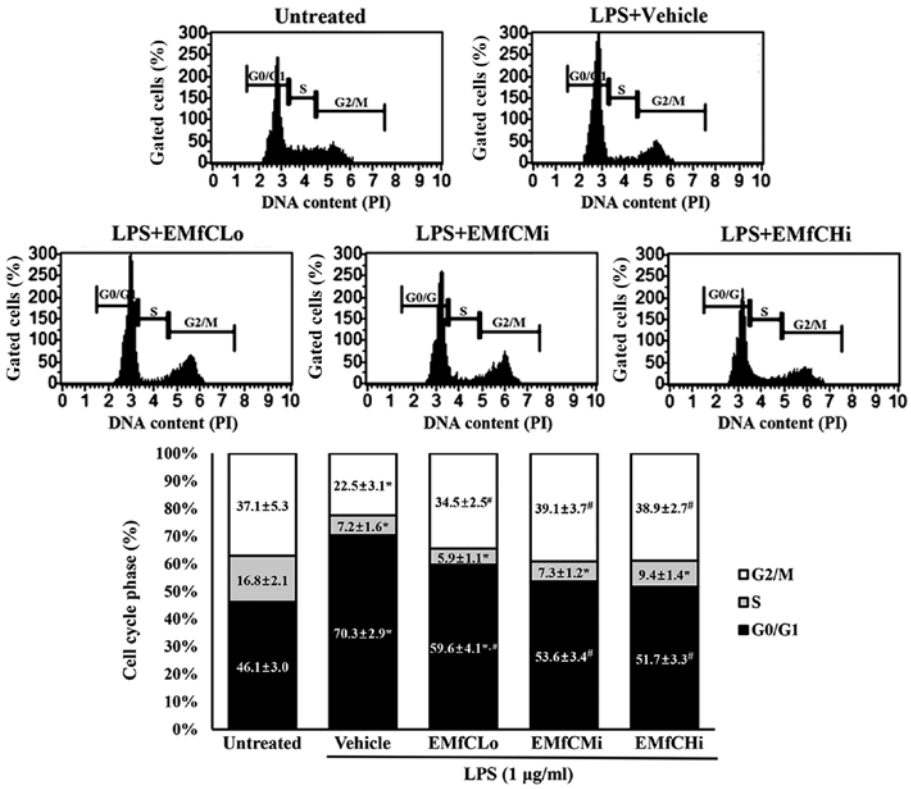

Figure 5. Detection of cell cycle arrest. PI staining was performed to determine the cell cycle distribution, by flow cytometric analysis of the DNA content of nuclei of EMfC+LPS-treated RAW264.7 cells. Following exposure to EMfC, the numbers of cells in the G_0/G_1, S and G_2/M stage were determined. For each group, two to three wells were used for PI staining, and the cell number at each phase was counted in duplicates for each sample. Data are presented as the mean ± SD. *P<0.05 vs. Untreated group; #P<0.05 vs. Vehicle+LPS treated group. PI, propidium iodide; EMfC, ethanol extracts of mulberry leaves fermented with *C. militaris*; LPS, lipopolysaccharide; Lo, low; Mi, medium; Hi, high.

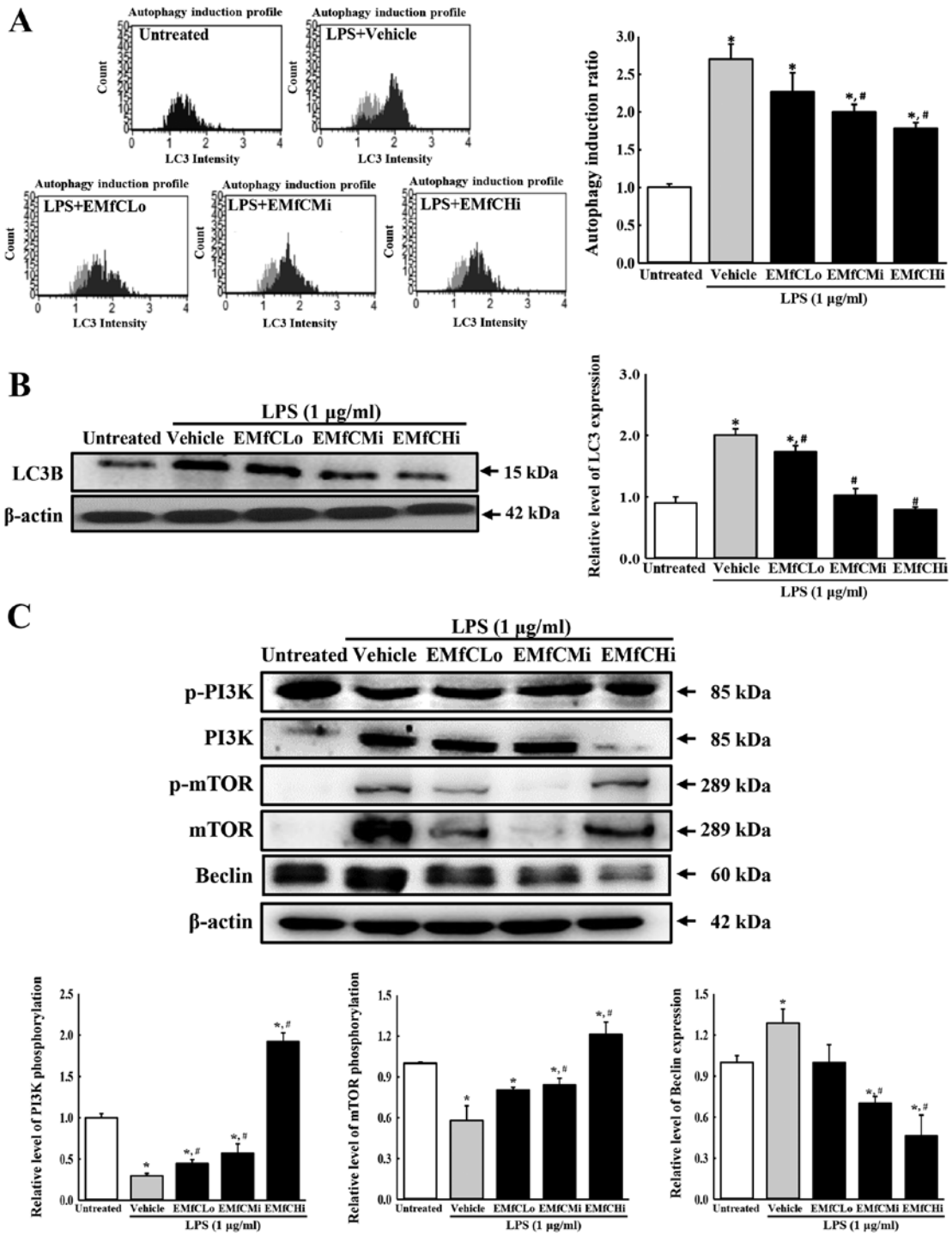

Figure 6. Detection of autophagic vacuole and PI3K/mTOR signaling pathway. (A) Autophagy induction profile and ratio. RAW264.7 cells were treated with EMfC+LPS for 24 h, washed and stained using the Autophagy LC3-antibody-based kit for FACS analysis. For each group, two to three dishes were used in the preparation of the LC3-stained cells, and FACS analysis was performed in duplicate for each sample. The autophagy induction ratio was presented as test sample fluorescence relative to control. (B) Expression levels of LC3B. Alterations in the levels of LC3 and β-actin proteins were measured by western blotting. (C) Expression levels of PI3K/mTOR signaling pathway members. Alterations in the levels of p-PI3K/PI3K, p-mTOR/mTOR, Beclin and β-actin proteins were measured by western blotting. After the intensity of each band was determined using an imaging densitometer, relative levels of the five proteins were calculated based on the intensity of actin protein. For each group, two to three dishes were used in the preparation of cell homogenates, and western blot analysis was performed in duplicate for each sample. Data are presented as the mean ± SD. *P<0.05 vs. Untreated group; #P<0.05 vs. Vehicle+LPS-treated group. EMfC, ethanol extracts of mulberry leaves fermented with *C. militaris*; LPS, lipopolysaccharide; p-, phosphorylated; FACS, fluorescence-activated cell sorting; Lo, low; Mi, medium; Hi, high.

of LPS and inflammatory factors such as NO and prostaglandin E2 (PGE2), and inflammatory cytokines such as TNF-α, IL-1β and IL-6 (26,36). These inflammatory factors and inflammatory cytokines are the main markers of inflammation (37). The inflammatory factor PEG2 (active oxygen species induced by COX-2) increases the permeability of blood vessels, resulting in fever, abscess and pain during the inflammatory process. In addition, inflammatory cytokines such as TNF-α, IL-1β and

IL-6 also cause fever, inflammation of endocardial cells, activation of neutrophils, increased breakdown of muscles and fats, and, in severe cases, septic shock (38). We therefore evaluated the inhibitory effect of EMfC on the production of inflammatory cytokines (TNF-α, IL-1β and IL-6) in LPS-stimulated RAW264.7 cells. Our results indicate that EMfC effectively and dose-dependently reduces the generation of inflammatory factors and inflammatory cytokines induced by LPS.

The MAPK pathway corresponds to the upstream region of the transcriptional factor NF-κB signal transduction, and is involved in the LPS-induced inflammatory response involving TLR4. It also regulates the growth and differentiation of cells, and controls the cell response to cytokines and stresses. Therefore, we investigated the MAPK pathway to determine the mechanism by which EMfC regulates the LPS-induced inflammatory response. As presented in Fig. 4, EMfC inhibits phosphorylation of ERK1/2, p38 MAPK and JNK of the MAPK pathway. Thus, although studies on NF-κB (the downstream signal transduction of MAPK) were not conducted, EMfC was observed to play a role in controlling MAPK, and it is assumed that EMFC also controls NF-κB. Future research needs to examine the mechanism of EMFC that controls NF-κB regulation. In addition, we examined LPS-induced cell cycle changes, to determine whether regulation of the MAPK pathway by EMfC is involved in cell growth and differentiation. Interestingly, we observed that the G1 arrest caused after exposure to LPS is restored by EMfC treatment.

Autophagy is the process that maintains cell homeostasis, and is an important catabolism for disassembling unnecessary or dysfunctional components of cells through the lysosome (39). It is a fundamental phenomenon in most tissues, and is also triggered by lack of sugars and amino acids in the cell, as well as by hypoxia, oxidative stress, and administration of chemotherapy agents (40). It has recently been reported that autophagy acts as an intermediary in diseases such as cancer and diabetes, as well as in inflammatory responses (40,41). In inflammation, autophagy helps to eliminate microbes in cells through phagocytosis, and the phagocytosis antigens are mainly involved in the presentation of major histocompatibility complex class II molecules. Autophagy is also reported to be involved in the inflammatory response, aiding the action of PAMP (cytosolic pathogen-associated molecule pattern) and TLR7 (42,43). In our study, we observed that EMfC exposure inhibits the LPS-induced autophagy. In addition, EMfC also inhibits phosphorylation of PI3K and mTOR, with a signal transduction that regulates autophagy and ultimately inhibiting the LPS-induced autophagy.

Our study has limitations, in that we did not investigate the protective effects of EMfC with high or low concentrations of LPS stimulation. In most previous studies, RAW264.7 cells were stimulated by LPS at 1 mg/ml, although only a few studies applied different concentrations (44-47). Based on previous studies, our study also established 1 mg/ml as the optimal concentration to evaluate the protective effects of EMfC. Moreover, this LPS concentration successfully reduced the viability of RAW264.7 cells by ~30% in our pilot study, where we had screened the cell viability at various concentration of LPS (data not shown). However, more studies are required to evaluate the protective effects of EMfC in cell models with higher or lower concentrations of LPS, although the protective effects of EMfC have been proven at optimum concentrations of LPS.

The results of this study reveal that EMfC prevents the inflammatory response and autophagy pathway in LPS-induced macrophages. This anti-inflammatory mechanism of EMfC is associated with the regulation of iNOS-mediated COX-2 induced pathway, expression of inflammatory cytokines, MAPK signaling pathway, and cell cycle progression. Furthermore, EMfC exposure inhibits the LPS-induced autophagy through activation of the PI3K/mTOR pathway. Taken together, our results indicate that EMfC has excellent anti-inflammatory and anti-autophagy capabilities, and is a competitive and potential drug candidate for inflammation-related diseases.

Acknowledgements

The authors would like to thank Miss Jin Hyang Hwang for directing the animal care and use at the Laboratory Animal Resources Center, Pusan National University (Miryang, Republic of Korea).

Funding

This study was supported by a grant from the Korea Institute of Planning Evaluation for Technology of Food, Agriculture, Forestry and Fisheries (grant no. 116027-032-HD030; to DYW).

Availability of data and materials

The datasets used and/or analyzed during the current study are available from the corresponding author on reasonable request.

Authors' contributions

MRL, JEK, JJP, JYC, BRS, DSK and DYH participated in designing the study, sample preparation, animal experiments and data analyses. YWC and KMK helped with sample preparation and data analysis. HKS majorly performed the first draft preparation and data analysis. DYH was a major contributor in experimental design, funding management and writing the manuscript. All authors read and approved the final manuscript.

Ethics approval and consent to participate

Not applicable.

Patient consent for publication

Not applicable.

Competing interests

The authors declare that they have no competing interests.

References

1. Luo A, Leach ST, Barres R, Hesson LB, Grimm MC and Simar D: The microbiota and epigenetic regulation of T helper 17/regulatory T cells: In search of a balanced immune system. Front Immunol 8: 417, 2017.

2. Hawiger J: Innate immunity and inflammation: A transcriptional paradigm. Immunol Res 23: 99-109, 2001.
3. Artis D and Spits H: The biology of innate lymphoid cells. Nature 517: 293-301, 2015.
4. Isailovic N, Daigo K, Mantovani A and Selmi C: Interleukin-17 and innate immunity in infections and chronic inflammation. J Autoimmun 60: 1-11, 2015.
5. Rock KL, Lai JJ and Kono H: Innate and adaptive immune response to cell death. Immunol Rev 243: 191-205, 2011.
6. Waisman A, Liblau RS and Becher B: Innate and adaptive immune responses in the CNS. Lancet Neurol 14: 945-955, 2015.
7. Beutler B, Krochin N, Milsark IW, Luedke C and Cerami A: Control of cachectin (tumor necrosis factor) synthesis: Mechanisms of endotoxin resistance. Science 232: 977-980, 1986.
8. Hou XL, Tong Q, Wang WQ, Shi CY, Xiong W, Chen J, Liu X and Fang JG: Suppression of inflammatory responses by dihydromyricetin, a flavonoid from ampelopsis grossedentata, via inhibiting the activation of NF-κB and MAPK signaling pathways. J Nat Prod 78: 1689-1696, 2015.
9. Kim HY, Hwang KW and Park SY: Extracts of *Actinidia arguta* stems inhibited LPS-induced inflammatory responses through nuclear factor-κB pathway in Raw 264.7 cells. Nutr Res 34: 1008-1016, 2014.
10. Flaczyk E, Kobus-Cisowska J, Przeor M, Korczak J, Remiszewski M, Korbas E and Buchowski M: Chemical characterization and antioxidative properties of Polish variety of *Morus alba* L. leaf aqueous extracts from the laboratory and pilot-scale processes. Agric Sci 4: 141-147, 2013.
11. Thanchanit T, Surawej N and Pornanong A: Mulberry leaves and their potential effects against cardiometabolic risks: A review of chemical compositions, biological properties and clinical efficacy. Pharm Biol 56: 109-118, 2018.
12. Gunjal S, Ankola AV and Bhat K: In vitro antibacterial activity of ethanolic extract of *Morus alba* leaf against pathogens. Indian J Dent Res 26: 533-536, 2015.
13. Raman ST, Ganeshan AK, Chen C, Jin C, Li SH, Chen HJ and Gui Z: *In vitro* and *in vivo* antioxidant activity of flavonoid extracted from mulberry fruit (*Morus alba* L.). Pharmacogn Mag 12: 128-133, 2016.
14. Wang Y, Xiang L, Wang C, Tang C and He X: Antidiabetic and antioxidant effects and phytochemicals of mulberry fruit (*Morus alba* L.) polyphenol enhanced extract. PLoS One 8: e71144, 2013.
15. Jo SP, Kim JK and Lim YH: Antihyperlipidemic effects of stilbenoids isolated from *Morus alba* in rats fed a high-cholesterol diet. Food Chem Toxicol 65: 213-218, 2014.
16. Chan EW, Lye PY and Wong SK: Phytochemistry, pharmacology, and clinical trials of *Morus alba*. Chin J Nat Med 14: 17-30, 2016.
17. Lee MR, Kim JE, Choi JY, Park JJ, Kim HR, Song BR, Choi YW, Kim KM, Song H and Hwang DY: Anti-obesity effect in high-fat-diet-induced obese C57BL/6 mice: Study of a novel extract from mulberry (*Morus alba*) leaves fermented with *Cordyceps militaris*. Exp Ther Med 17: 2185-2193, 2019.
18. Lee MR, Bae SJ, Kim JE, Song BR, Choi JY, Park JJ, Park JW, Kang MJ, Choi HJ, Choi YW, *et al*: Inhibition of endoplasmic reticulum stress in high-fat-diet-induced obese C57BL/6 mice: Efficacy of a novel extract from mulberry (*Morus alba*) leaves fermented with *Cordyceps militaris*. Lab Anim Res 34: 288-294, 2018.
19. De Silva DD, Rapior S, Sudarman E, Stadler M, Xu J, Alias SA and Hyde KD: Bioactive metabolites from macrofungi: Ethnopharmacology, biological activities and chemistry. Fungal Divers 62: 1-40, 2013.
20. Silva DD, Rapior S, Fons F, Bahkali AH and Hyde KD: Medicinal mushrooms in supportive cancer therapies: An approach to anti-cancer effects and putative mechanisms of action. Fungal Divers 55: 1-35, 2012.
21. Kim JR, Yeon SH, Kim HS and Ahn YJ: Larvicidal activity against *plutella xylostella* of cordycepin form fruiting body of *Cordyceps militaris*. Pest Manag Sci 58: 713-717, 2012.
22. Ramesh T, Yoo SK, Kim SW, Hwang SY, Sohn SH, Kim IW and Kim SK: Cordycepin (3'-deoxyadenosine) attenuates age-related oxidative stress and ameliorates antioxidant capacity in rats. Exp Gerontol 47: 979-987, 2012.
23. Hung YP and Lee CL: Higher anti-liver fibrosis effect of *Cordyceps militaris*-fermented product cultured with deep ocean water via inhibiting proinflammatory factors and fibrosis-related factors expressions. Mar Drugs 15: 168, 2017.
24. Oh H, Ko EK, Kim DH, Jang KK, Park SE, Lee HS and Kim YC: Secoiridoid glucosides with free radical scavenging activity from the leaves of *Syringa dilatate*. Phytother Res 17: 417-419, 2003.
25. Sun J, Zhang X, Broderick M and Fein H: Measurement of nitric oxide production in biological systems by using griess reaction assay. Sensors 3: 276-284, 2003.
26. Choi EA, Park HY, Yoo HS and Choi YH: Anti-inflammatory effects of egg white combined with chalcanthite in lipopolysaccharide-stimulated BV2 microglia through the inhibition of NF-κB, MAPK and PI3K/Akt signaling pathways. Int J Mol Med 31: 134-162, 2012.
27. Livak KJ and Schmittgen TD: Analysis of relative gene expression data using real-time quantitative PCR and the 2(-Delta C(T)) method. Methods 25: 402-408, 2001.
28. Prescott LM, Harley JP and Klein DA: Microbiology. 6th edition. McGraw-Hill, New York, NY, 2006.
29. Trinh HT, Han SJ, Kim SW, Lee YC and Kim DH: Bifidus fermentation increases hypolipidemic and hypoglycemic effects of red ginseng. J Microbiol Biotechnol 17: 1127-1133, 2007.
30. Kim YJ and Park WS: Anti-inflammatory effect of quercetin on RAW 264.7 mouse macrophages induced with polyinosinic-polycytidylic acid. Molecules 21: 450, 2016.
31. Song MH, Bae JT, Ko HJ, Jang TM, Lee JD, Lee GS and Pyo HB: Anti-oxidant effect and anti-inflammatory of fermented *Citrus Unshiu* peel extract by using *Schizophyllum commune*. J Soc Cosmet Sci Korea 37: 351-356, 2011.
32. Liu RL, Ren SF and Wang YZ: Influence of the fermentation *Cordyceps sinensisfy* powder on blood uric acid and lipid in the cases of essential hypertension. World Clin Drugs 27: 498-502, 2006.
33. Choi EM and Hwang JK: Effects of *Morus alba* leaf extract on the production of nitric oxide, prostaglandin E2 and cytokines in RAW264.7 macrophages. Fitoterapia 76: 608-613, 2005.
34. John JH: Antioxidant and prooxidant mechanisms in the regulation of redox(y)-sensitive transcription factors. Cell Signal 14: 879-897, 2002.
35. Ohshima H and Bartsch H: Chronic infections and inflammatory processes as cancer risk factors: Possible role of nitric oxide in carcinogenesis. Mutat Res 305: 253-264, 1994.
36. Muniandy K, Gothai S, Badran KMH, Suresh Kumar S, Esa NM and Arulselvan P: Suppression of proinflammatory cytokines and mediators in LPS-induced RAW 264.7 macrophages by stem extract of *alternanthera sessilis* via the inhibition of the NF-κB pathway. J Immunol Res 2018: 3430684, 2018.
37. Lin HI, Chu SJ, Wang D and Feng NH: Pharmacological modulation of TNF production in macrophages. J Microbiol Immunol Infect 37: 8-15, 2004.
38. Abbas A, Lichtman A and Pillai S: Cellular and Molecular Immunology 6th edition. Seoul, pp271-296, 2008.
39. Cuervo AM: Autophagy: In sickness and in health. Trends Cell Biol 14: 70-77, 2004.
40. Sridhar S, Botbol Y, Macian F and Cuervo AM: Autophagy and disease: Always two sides to a problem. J Pathol 226: 255-273, 2012.
41. Kim J, Kundu M, Viollet B and Guan KL: AMPK and mTOR regulate autophagy through direct phosphorylation of Ulk1. Nat Cell Biol 13: 132-141, 2011.
42. Deretic V: Multiple regulatory and effector roles of autophagy in immunity. Curr Opin Immunol 21: 53-62, 2009.
43. Orvedahl A and Levine B: Eating the enemy within: Autophagy in infectious diseases. Cell Death Differ 16: 57-69, 2009.
44. Xu J, Zhao Y and Aisa HA: Anti-inflammatory effect of pomegranate flower in lipopolysaccharide (LPS)-stimulated RAW264.7 macrophages. Pharm Biol 55: 2095-2101, 2017.
45. Sugiyama Y, Hiraiwa Y, Hagiya Y, Nakajima M, Tanaka T and Ogura SI: 5-Aminolevulinic acid regulates the immune response in LPS-stimulated RAW 264.7 macrophages. BMC Immunol 19: 41, 2018.
46. Dong J, Li J, Cui L, Wang Y, Lin J, Qu Y and Wang H: Cortisol modulates inflammatory responses in LPS-stimulated RAW264.7 cells via the NF-κB and MAPK pathways. BMC Vet Res 14: 30, 2018.
47. Lee DS, Hwang IH, Im NK, Jeong GS and Na MK: Anti-inflammatory effect of dactyloquinone B and cyclospongiaquinone-1 mixture in RAW264.7 macrophage and ICR mice. Nat Prod Sci 21: 268-272, 2015.